Energy cascades in the convective atmospheric boundary layer: analysis of structure functions

Jakub. L. Nowak[1], Marta Wacławczyk[1], John C. Vassilicos[2], Stanisław Król[1], Szymon P. Malinowski[1]

[1]Institute of Geophysics, Faculty of Physics, University of Warsaw, Poland

[2]Univ. Lille, CNRS, ONERA, Arts et Metiers Institute of Technology, Centrale Lille, UMR 9014 –LMFL – Laboratoire de Mécanique des Fluides de Lille – Kampé de Fériet, Lille, France

LTP 2023 collaboration

Turbulence cascade in the atmosphere

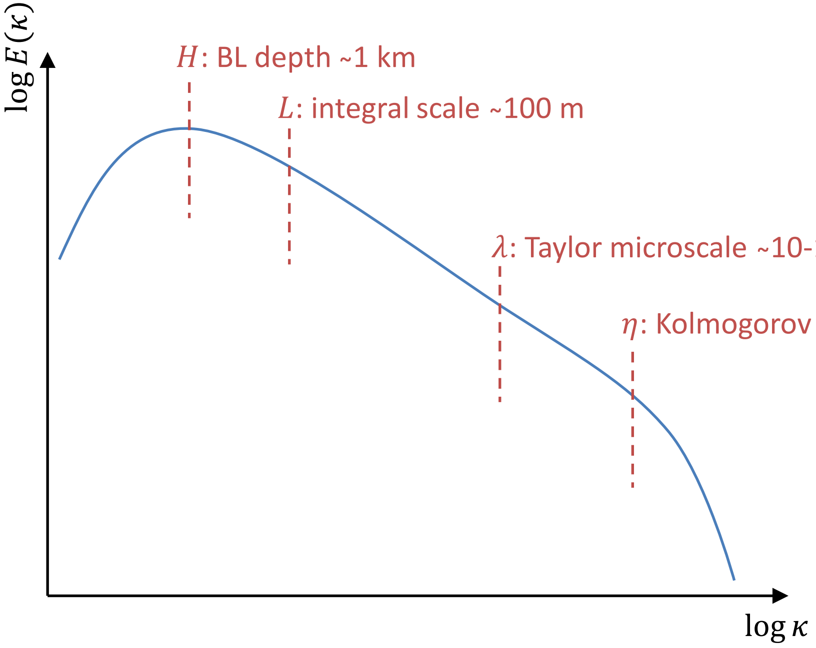

$$\overline{\delta u^2} \sim (\epsilon r)^{\frac{2}{3}}$$

$$\overline{\delta u^3} = -\frac{4}{5}\epsilon r \quad ?$$

$$\overline{\delta u \delta T} = 0 \quad ?$$

Field campaign EUREC4A 2020

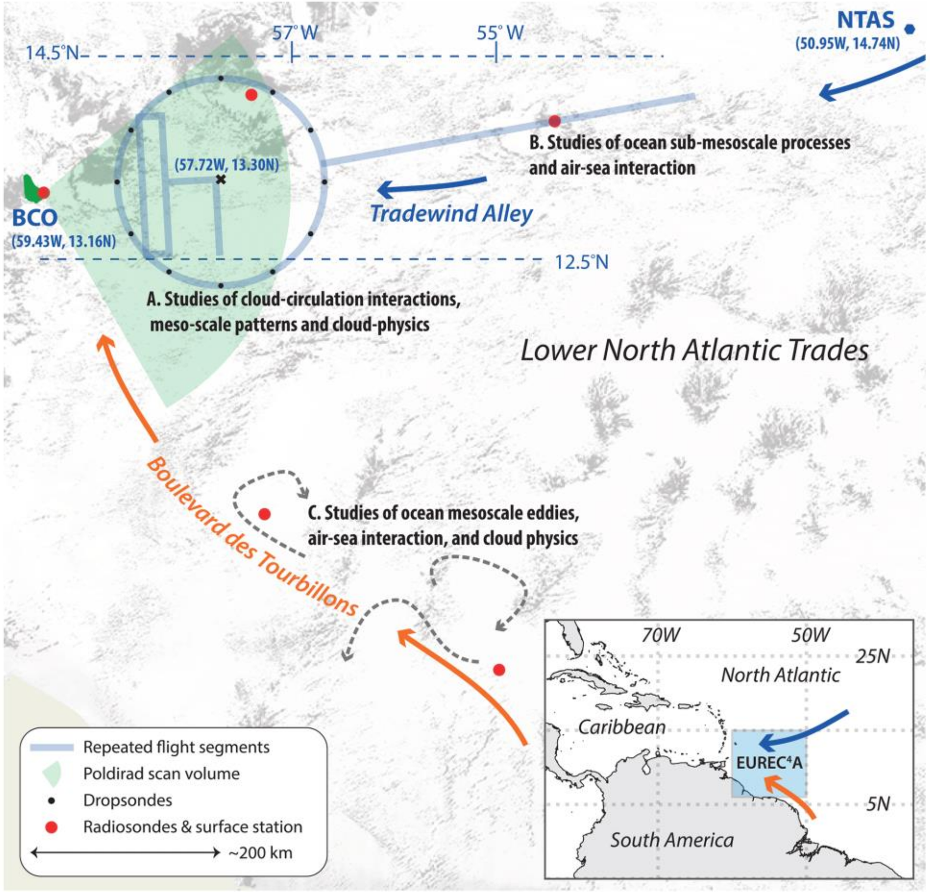

Elucidating the role of clouds–circulation coupling in climate

Jan-Feb 2020 in western Atlantic

French research aircraft SAFIRE ATR-42 (19 flights x 4 h)

Stevens et al. 2021, Bony et al. 2022

Trade winds

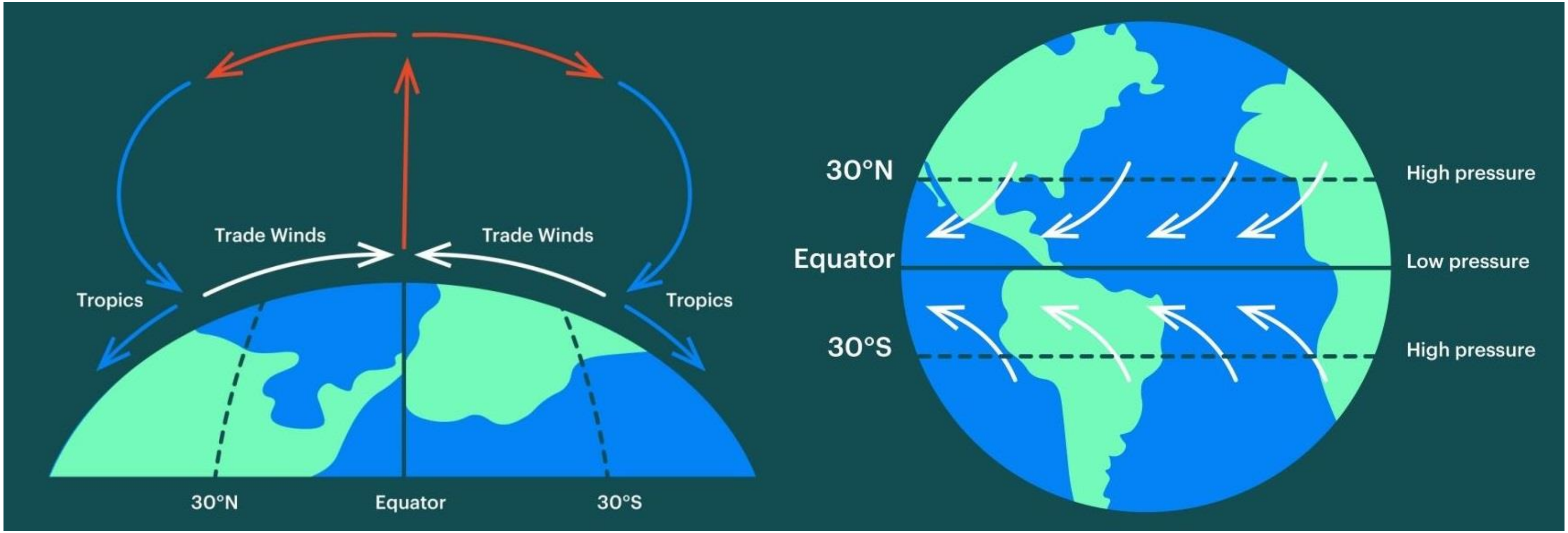

Valerya Milovanova / Windy.app

Shallow trade-wind convection

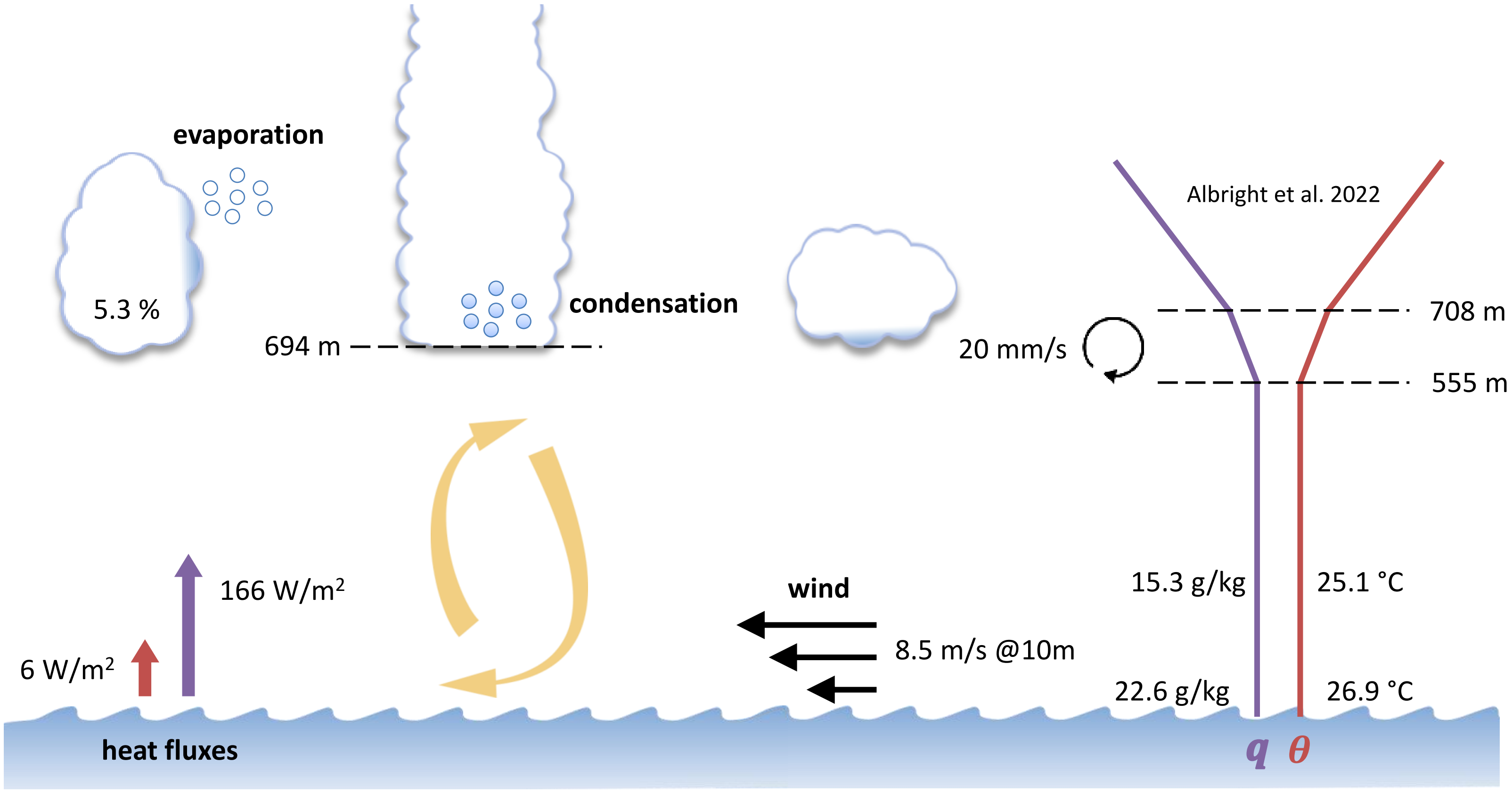

Research flights during EUREC4A

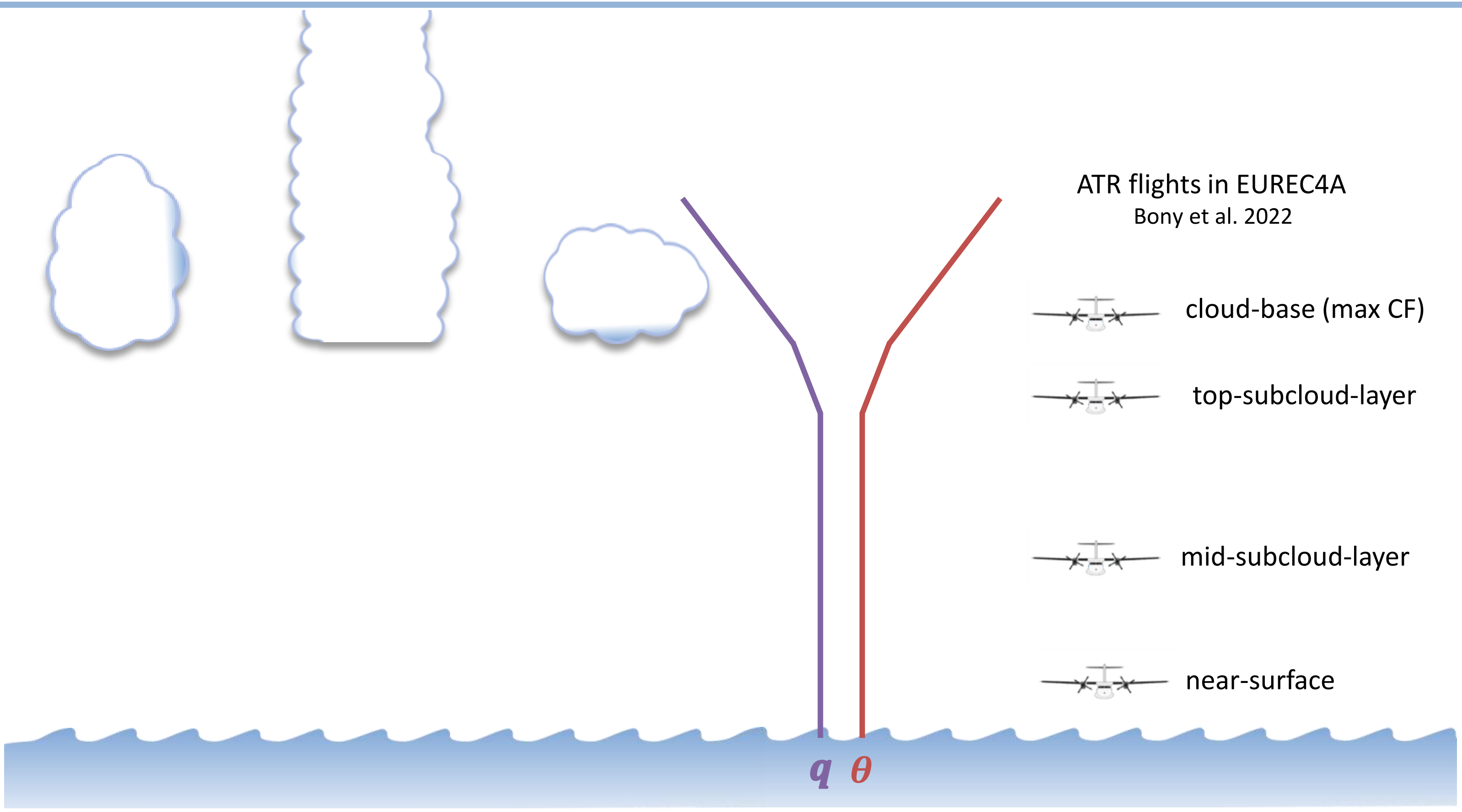

Flight segments

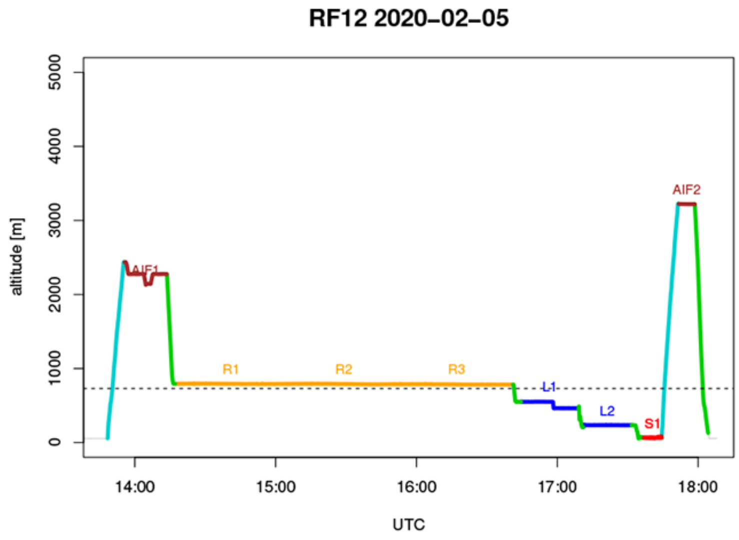

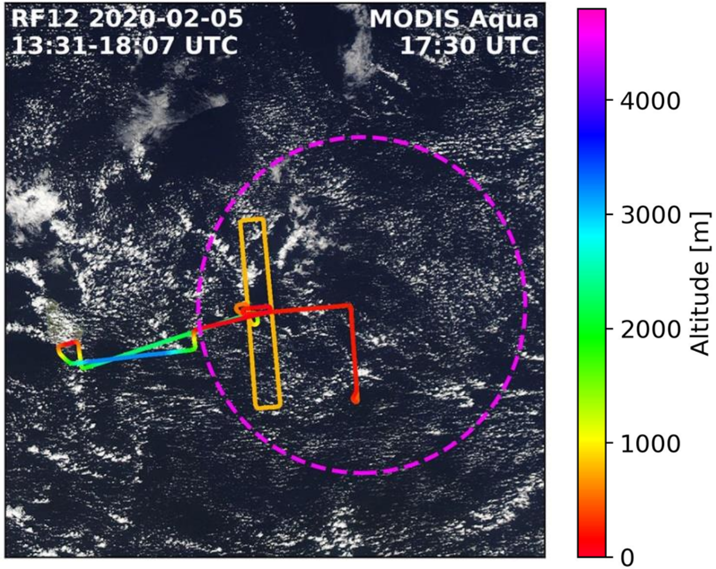

Bony et al. 2022, Brilouet et al. 2021

Level	#	Length [km]	Altitude [m]
cloud-base	114	54 (5)	807 (83)
top-subcloud	18	62 (10)	595 (47)
mid-subcloud	16	54 (7)	292 (27)
near-surface	9	40 (6)	64 (2)

Average values with std among segments given in parentheses.

Selected instrumentation

Instrument	Brief description	Position on ATR	
5-hole radome	For measuring the differential pressure around the nose of the aircraft	radome	
Pitot probes	Rosemount and Thales transducers connected to Pitot probes measuring static and dynamic pressure	fuselage	
Fine wire	fine wire resistance for measuring fast temperature fluctuations	nose (left-hand side)	
Licor 7500A	Near-infrared gas analyzer for measuring rapid humidity fluctuations	window (left-hand side)	
KH20	Campbell krypton hygrometer for measuring rapid humidity fluctuations	nose (left-hand side)	

Adapted from Bony et al. 2022

$$\frac{100\ \mathrm{m/s}}{25\ \mathrm{Hz}} = 4\ \mathrm{m}$$

$$\frac{50\ \mathrm{km} \cdot 25\ \mathrm{Hz}}{100\ \mathrm{m/s}} = 12\,500\ \text{samples}$$

Scale-by-scale budget derivation (1)

$B = g \frac{\theta_v - \widetilde{\theta_v}}{\widetilde{\theta_v}}$ buoyancy

$\theta_v = \theta(1 + 0.61 q_v)$ virtual potential temperature

$\theta = T \left(\frac{p_0}{p}\right)^{R_d/c_p}$ potential temperature

T: temperature, q_v: water vapor mass fraction, p: pressure, $p_0 = 1000$ hPa

$$B = g \frac{\theta - \tilde{\theta}}{\widetilde{\theta_v}} + 0.61 g \frac{\theta q_v - \widetilde{\theta q_v}}{\widetilde{\theta_v}}$$

B_θ B_q

Incompressible Boussinesq approximation

$$\partial_t \boldsymbol{u} + \boldsymbol{u} \cdot \nabla \boldsymbol{u} = \nabla \pi + \nu \nabla^2 \boldsymbol{u} + \boldsymbol{k} B$$

$$\partial_t B + \boldsymbol{u} \cdot \nabla B = \nu \nabla^2 B$$

$$\nabla \cdot \boldsymbol{u} = 0$$

$\pi = \frac{p}{\rho}$, ρ: reference density, $\boldsymbol{u} = (u, v, w)$

Scale-by-scale budget derivation (2)

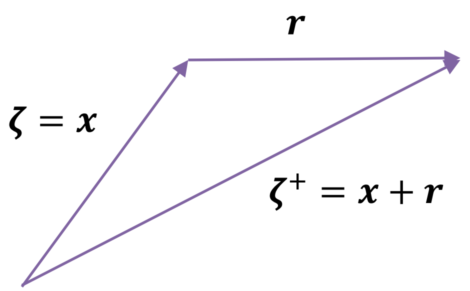

$$\boldsymbol{X} = \frac{1}{2}(\boldsymbol{\zeta} + \boldsymbol{\zeta}^{+})$$

$$\delta\boldsymbol{u}(\boldsymbol{X},\boldsymbol{r}) = \boldsymbol{u}(\boldsymbol{\zeta}^{+}) - \boldsymbol{u}(\boldsymbol{\zeta})$$

$$\delta B(\boldsymbol{X},\boldsymbol{r}) = B(\boldsymbol{\zeta}^{+}) - B(\boldsymbol{\zeta})$$

$$\delta\pi(\boldsymbol{X},\boldsymbol{r}) = \pi(\boldsymbol{\zeta}^{+}) - \pi(\boldsymbol{\zeta})$$

$$\frac{\partial|\delta\boldsymbol{u}|^2}{\partial t} + \nabla_{\boldsymbol{X}}\cdot\boldsymbol{u}_{\boldsymbol{X}}|\delta\boldsymbol{u}|^2 + \nabla_{\boldsymbol{r}}\cdot\delta\boldsymbol{u}|\delta\boldsymbol{u}|^2 = -2\nabla_{\boldsymbol{X}}\cdot\delta\boldsymbol{u}\delta\pi + \frac{\nu}{2}\nabla_{\boldsymbol{X}}^2|\delta\boldsymbol{u}|^2 + 2\nu\nabla_{\mathbf{r}}^2|\delta\boldsymbol{u}|^2 - 2\epsilon^{+} - 2\epsilon + 2\delta B\delta w$$

horizontal homogeneity + stationarity

$$\frac{\partial}{\partial z}\overline{w_{\boldsymbol{X}}|\delta\boldsymbol{u}|^2} + \nabla_{r}\cdot\overline{\delta\boldsymbol{u}|\delta\boldsymbol{u}|^2} = -2\frac{\partial}{\partial z}\overline{\delta w\delta\pi} + 2\nu\nabla_{\mathbf{r}}^2\overline{|\delta\boldsymbol{u}|^2} - 4\bar{\epsilon} + 2\overline{\delta B\delta w}$$

Valente and Vassilicos 2015

Scale-by-scale budget derivation (3)

$$2\overline{\delta B \delta w} - \nabla_r \cdot \overline{\delta \boldsymbol{u}|\delta \boldsymbol{u}|^2} - \frac{\partial}{\partial z}\overline{w_{\boldsymbol{X}}|\delta \boldsymbol{u}|^2} - 2\frac{\partial}{\partial z}\overline{\delta w \delta \pi} = 4\bar{\epsilon}$$

local averaging over r-sphere

$$W(r) = \frac{6}{4\pi r^3}\int_{|\boldsymbol{\rho}|\leq r} d^3\rho \overline{\delta B \delta w} \qquad S_3(r) = \frac{3}{4\pi}\int d\Omega_r \overline{\hat{\boldsymbol{r}} \cdot \delta \boldsymbol{u}|\delta \boldsymbol{u}|^2}$$

$$T(r) = \frac{3}{4\pi r^3}\frac{\partial}{\partial z}\int_{|\boldsymbol{\rho}|\leq r} d^3\rho\left(\overline{w_{\boldsymbol{X}}|\delta \boldsymbol{u}|^2} + 2\overline{\delta w \delta \pi}\right)$$

$$W - \frac{S_3}{r} - T = 4\bar{\epsilon}$$

Valente and Vassilicos 2015

Scale-by-scale budget equation

$$W - \frac{S_3}{r} - T = 4\bar{\epsilon}$$

$$W(r) = \frac{6}{4\pi r^3}\int_{|\boldsymbol{\rho}|\le r} d^3\rho\,\overline{\delta B \delta w}$$

$$S_3(r) = \frac{3}{4\pi}\int d\Omega_r \overline{\hat{\boldsymbol{r}}\cdot\delta\boldsymbol{u}|\delta\boldsymbol{u}|^2}$$

$$T(r) = \frac{3}{4\pi r^3}\frac{\partial}{\partial z}\int_{|\boldsymbol{\rho}|\le r} d^3\rho\left(\overline{w_X|\delta\boldsymbol{u}|^2} + 2\overline{\delta w \delta\pi}\right)$$

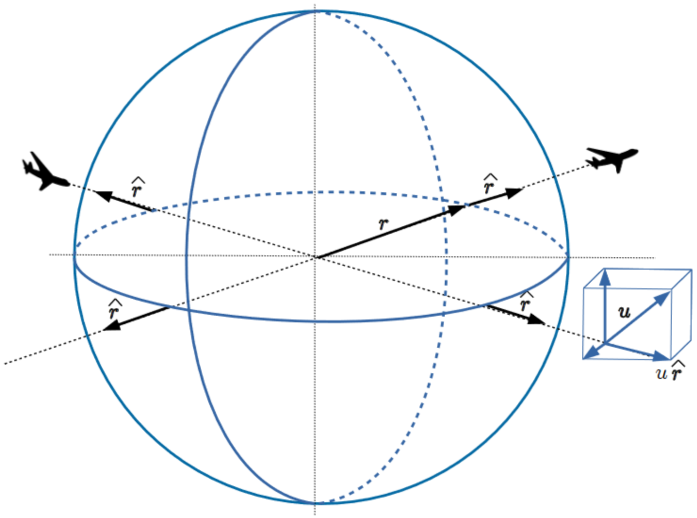

Approximation with measured quantities

$$W - \frac{S_3}{r} - T = 4\bar{\epsilon}$$

$$W(r) \approx \frac{6}{r^3}\int_0^r d\rho\rho^2\overline{\delta B \delta w} = W_\theta + W_q$$

$$S_3(r) \approx 3\overline{\delta u|\delta \boldsymbol{u}|^2}$$

$$T(r) \approx \frac{3}{r^3}\frac{\partial}{\partial z}\int_0^r d\rho\rho^2\left(\overline{w_X|\delta \boldsymbol{u}|^2} + 2\overline{\delta w \delta \pi}\right) = T_u + T_p$$

$$S_2(r) = C(\bar{\epsilon} r)^{\frac{2}{3}}$$

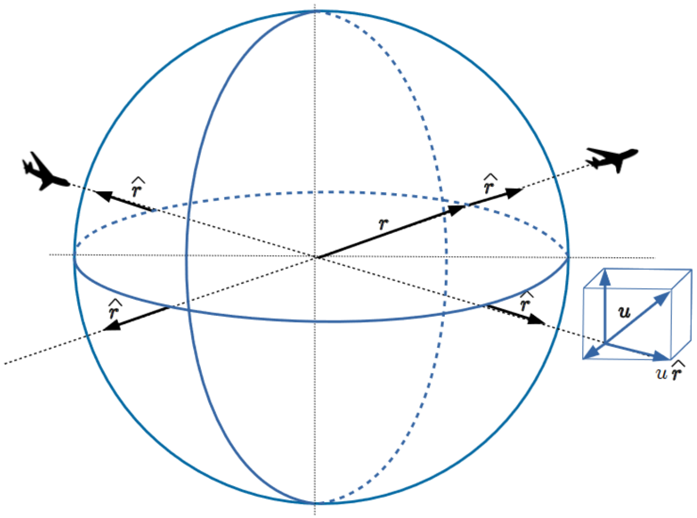

Buoyancy forcing

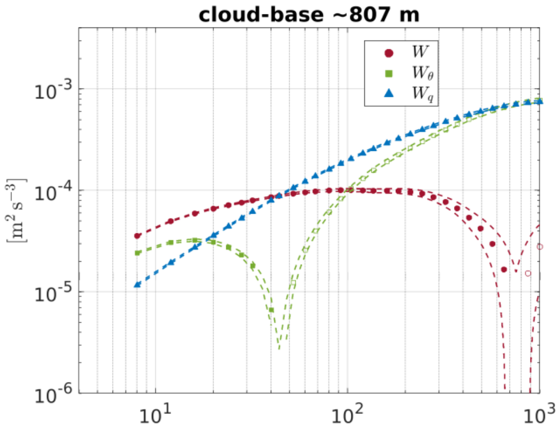

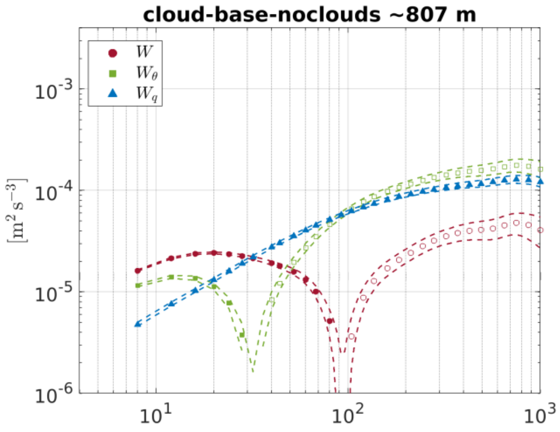

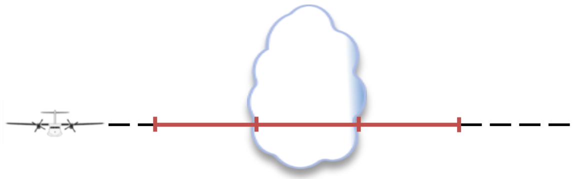

$LWC > 0.01\,\frac{\mathrm{g}}{\mathrm{m}^3}$ (1 Hz)

$RH > 98\ \%$ (25 Hz)

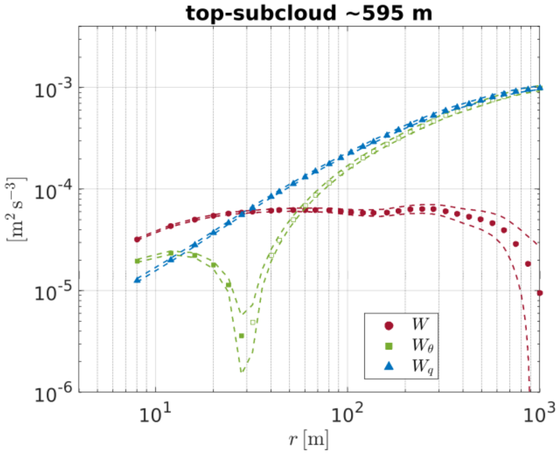

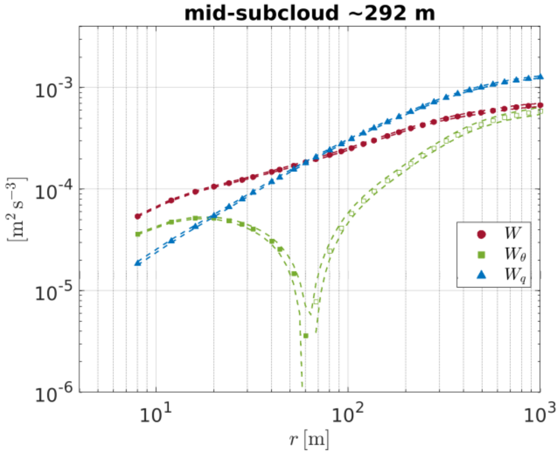

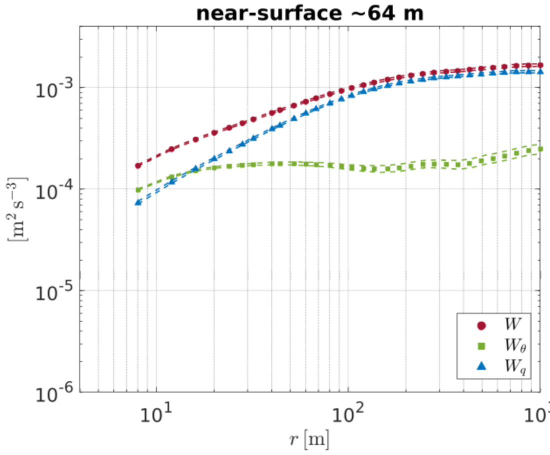

Nonlinear interscale transfer

S_3/r

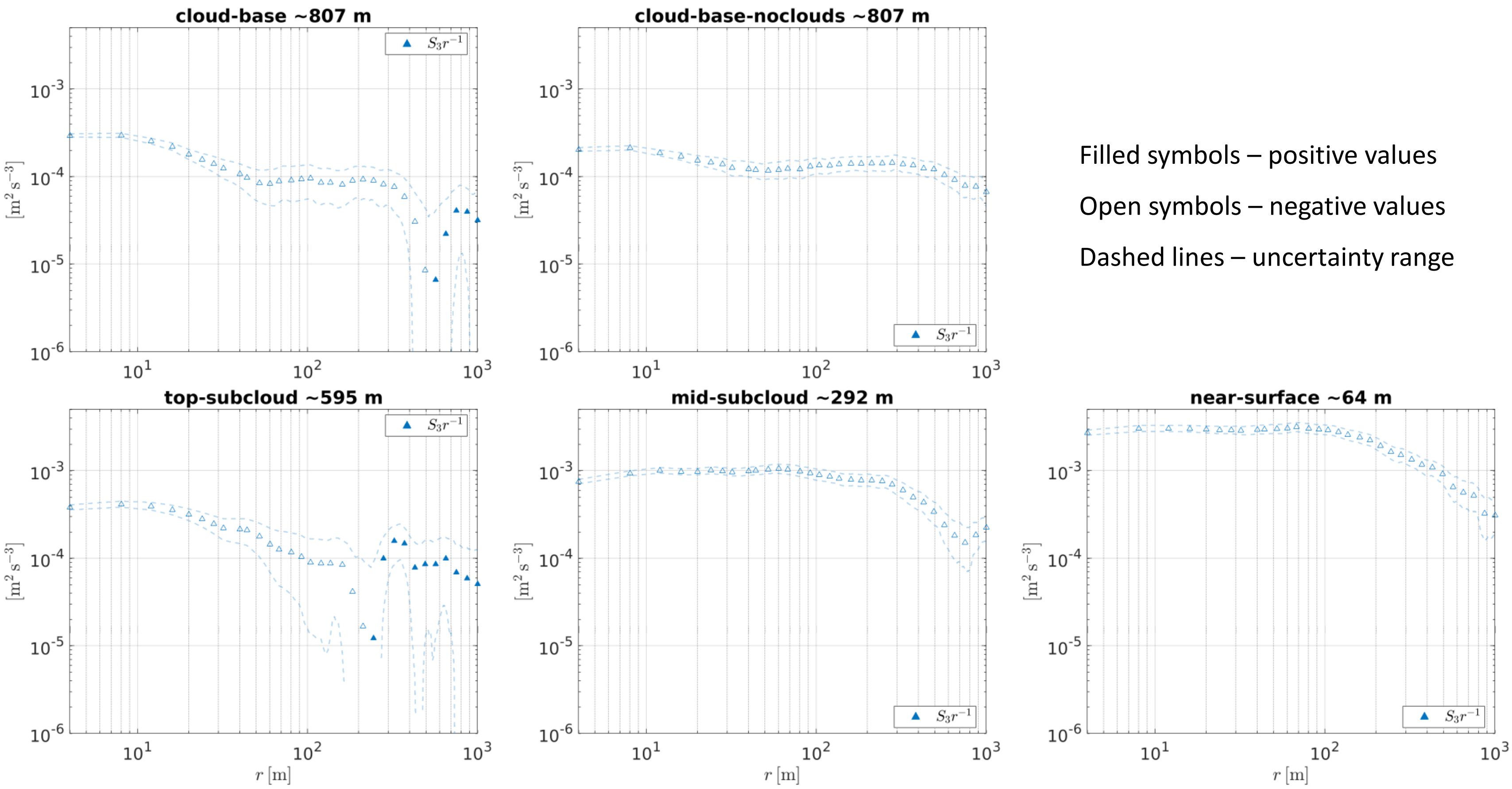

Filled symbols – positive values

Open symbols – negative values

Dashed lines – uncertainty range

Interspace transport

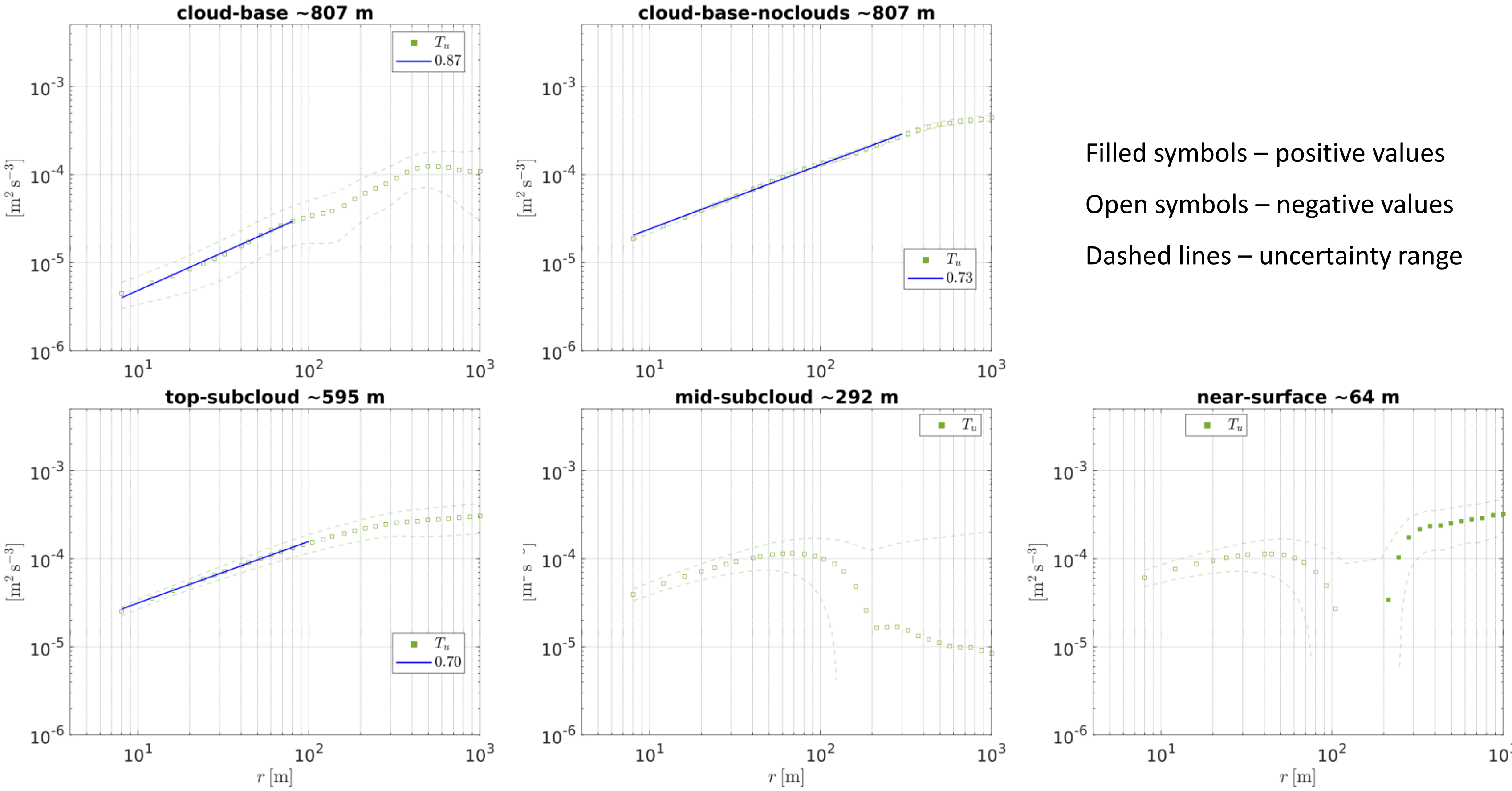

Filled symbols – positive values

Open symbols – negative values

Dashed lines – uncertainty range

Budget terms

$W - S_3/r - T = 4\bar{\epsilon}$

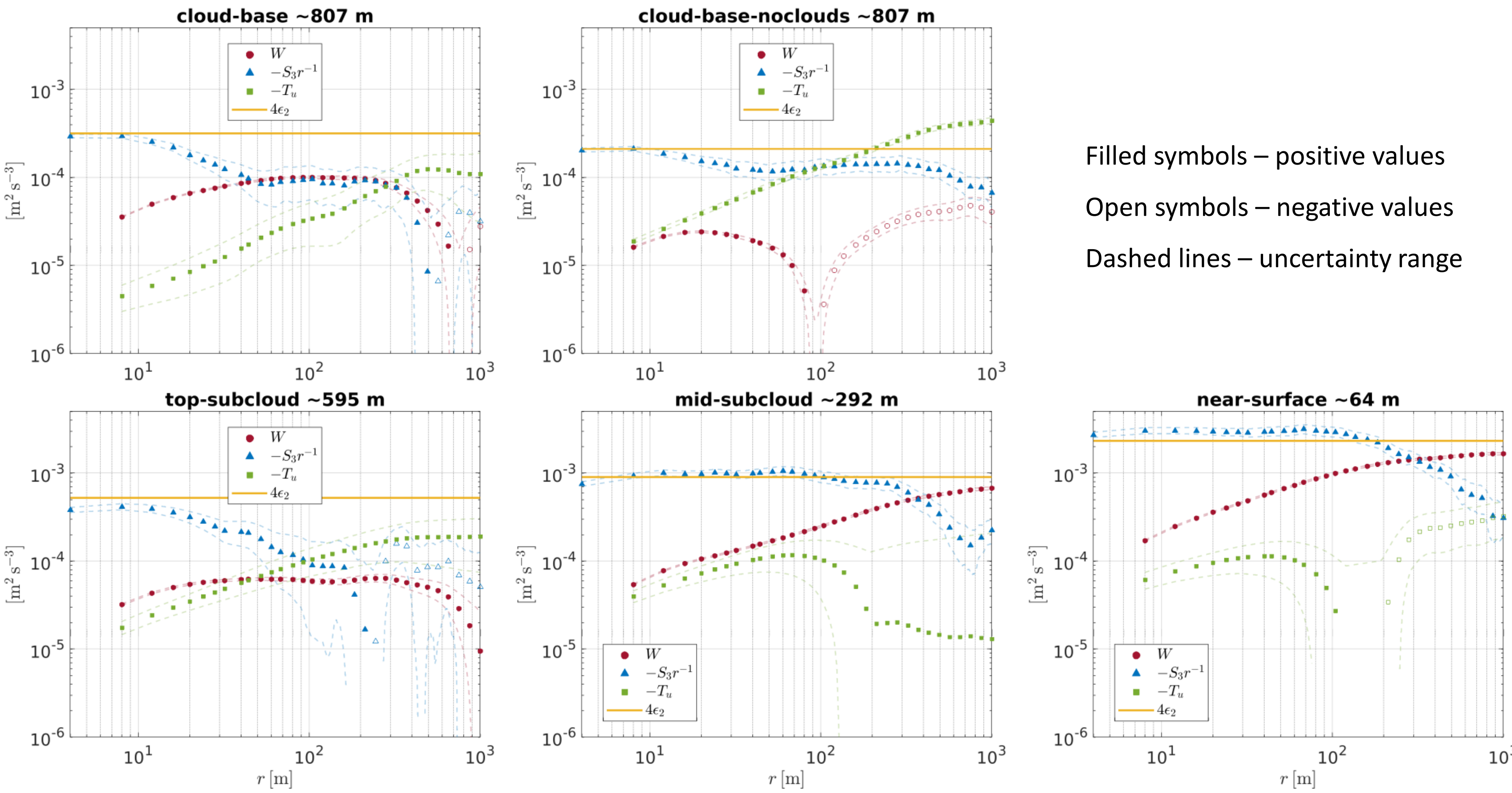

Filled symbols – positive values

Open symbols – negative values

Dashed lines – uncertainty range

Total budget

$W - S_3/r - T = 4\bar{\epsilon}$

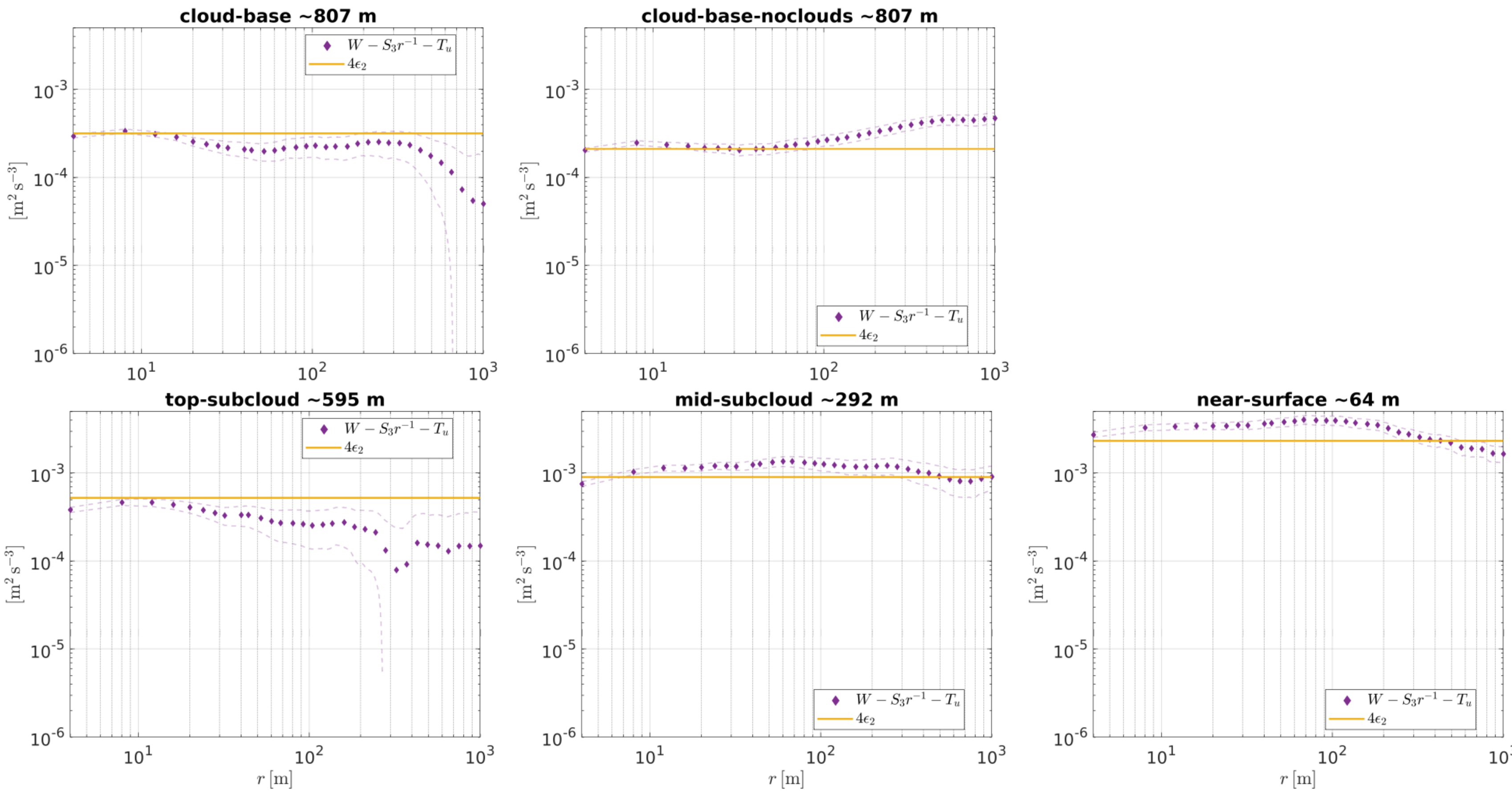

Idealized budgets

Equilibrium cascade
(near-surface and mid-subcloud)

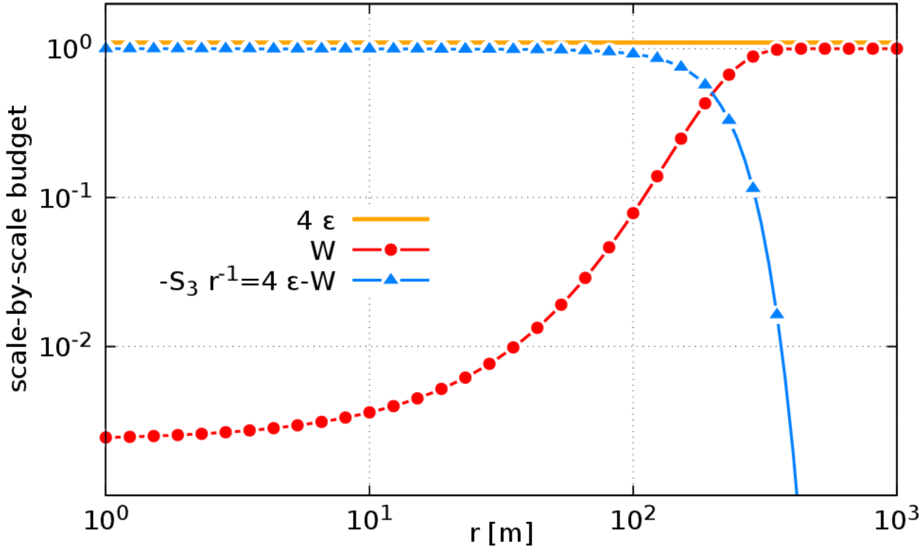

Non-equilibrium cascade
(top-subcloud and cloud-base)

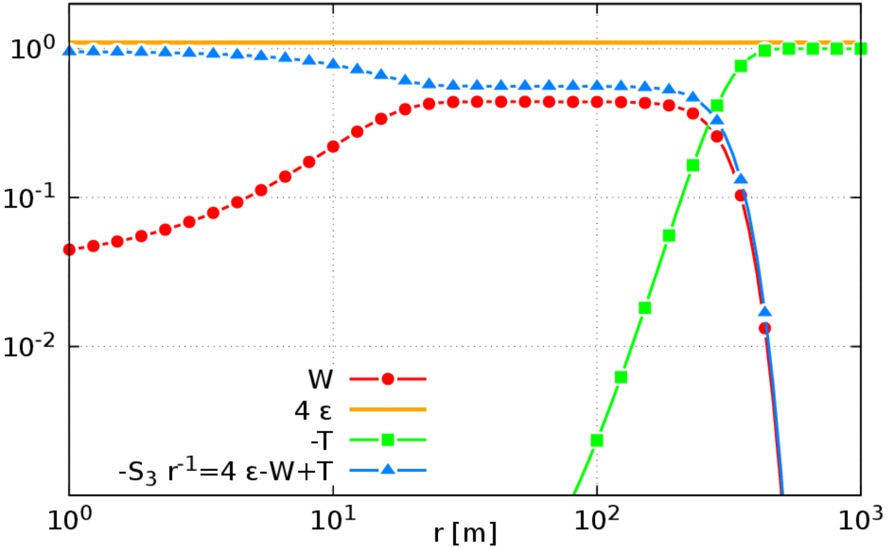

Conclusions

- Airborne in-situ measurements in shallow trade-wind regime of atmospheric boundary layer over ocean are used to investigate the scale-by-scale budget of turbulence kinetic energy.
- The budget involving buoyancy forcing, nonlinear interscale transfer, interspace transport and dissipation is approximately closed up to $\sim$200 m.
- At the near-surface and mid-subcloud levels, Kolmogorov equilibrium is observed over a range of scales from a few to above 100 m.
- At the top-subcloud and cloud-base levels, the budget is far from Kolmogorov equilibrium at scales above 10 m, with significant contribution of buoyancy forcing and turbulent transport. Buoyancy produces turbulence at intermediate scales while at large scales the stable stratification consumes part of the energy which is supposedly supplied by the transport from below.
- The contribution to the buoyancy forcing related to humidity variations is substantial and strictly positive at all levels. Almost always, it dominates over the contribution related to temperature only.

Energy cascades in the convective atmospheric boundary layer - summary

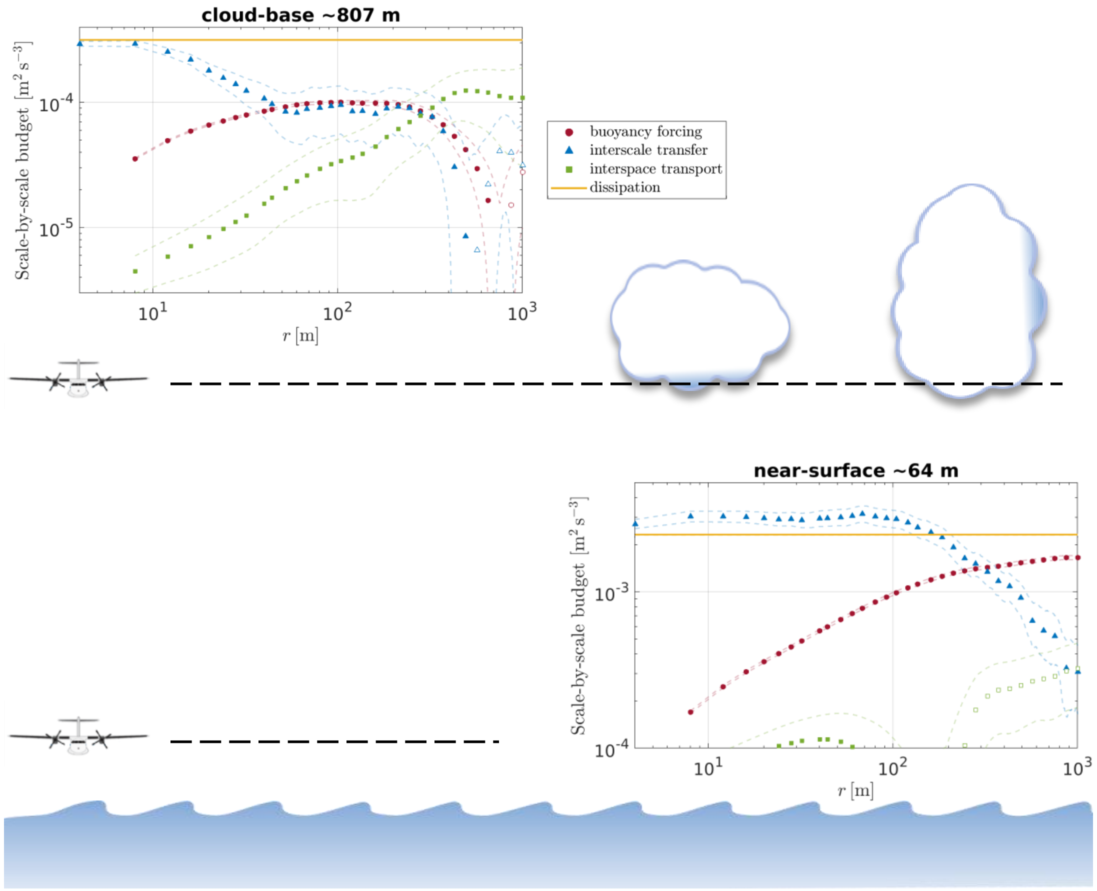

Jakub. L. Nowak[1], Marta Wacławczyk[1], John C. Vassilicos[2], Stanisław Król[1], Szymon P. Malinowski[1]

[1]Institute of Geophysics, Faculty of Physics, University of Warsaw, Poland

[2]Univ. Lille, CNRS, ONERA, Arts et Metiers Institute of Technology, Centrale Lille, UMR 9014 –LMFL – Laboratoire de Mécanique des Fluides de Lille – Kampé de Fériet, Lille, France

LTP 2023 collaboration

2nd order structure functions

$S_2/Cr^{2/3}$

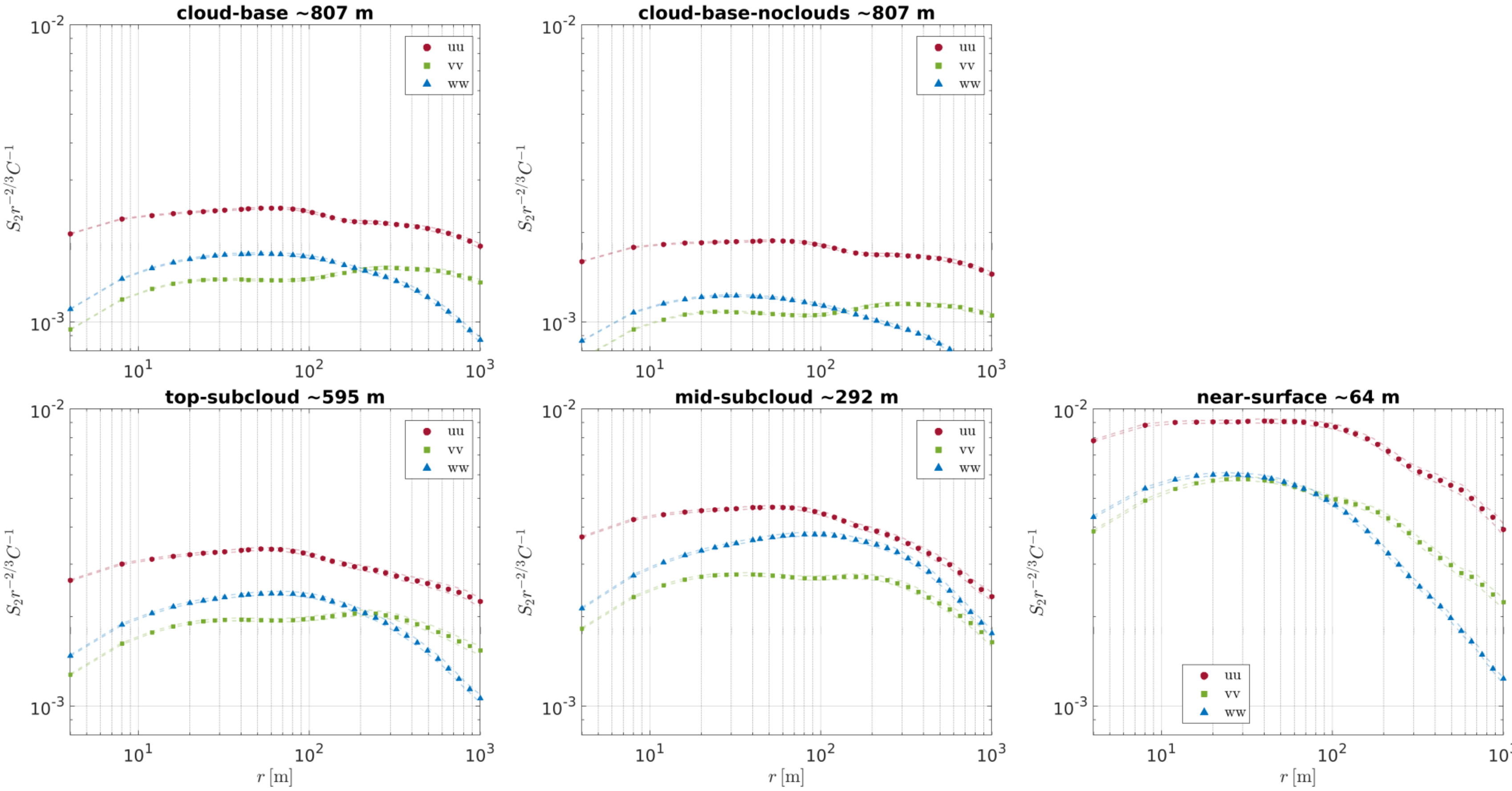

Dissipation rate

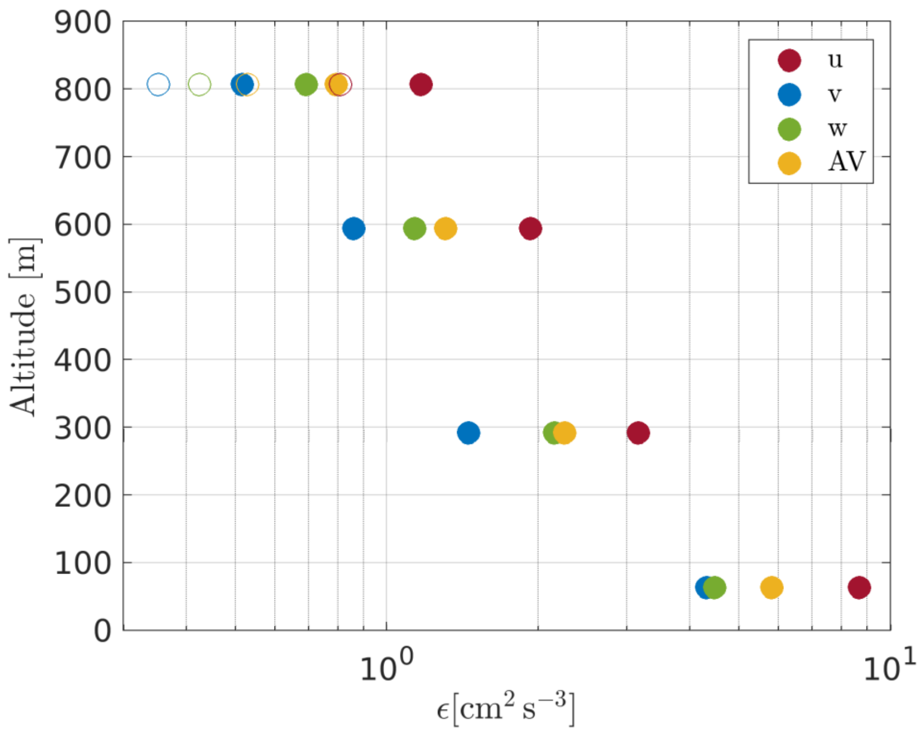

Open symbols - clouds excluded

Budget terms in linear scale

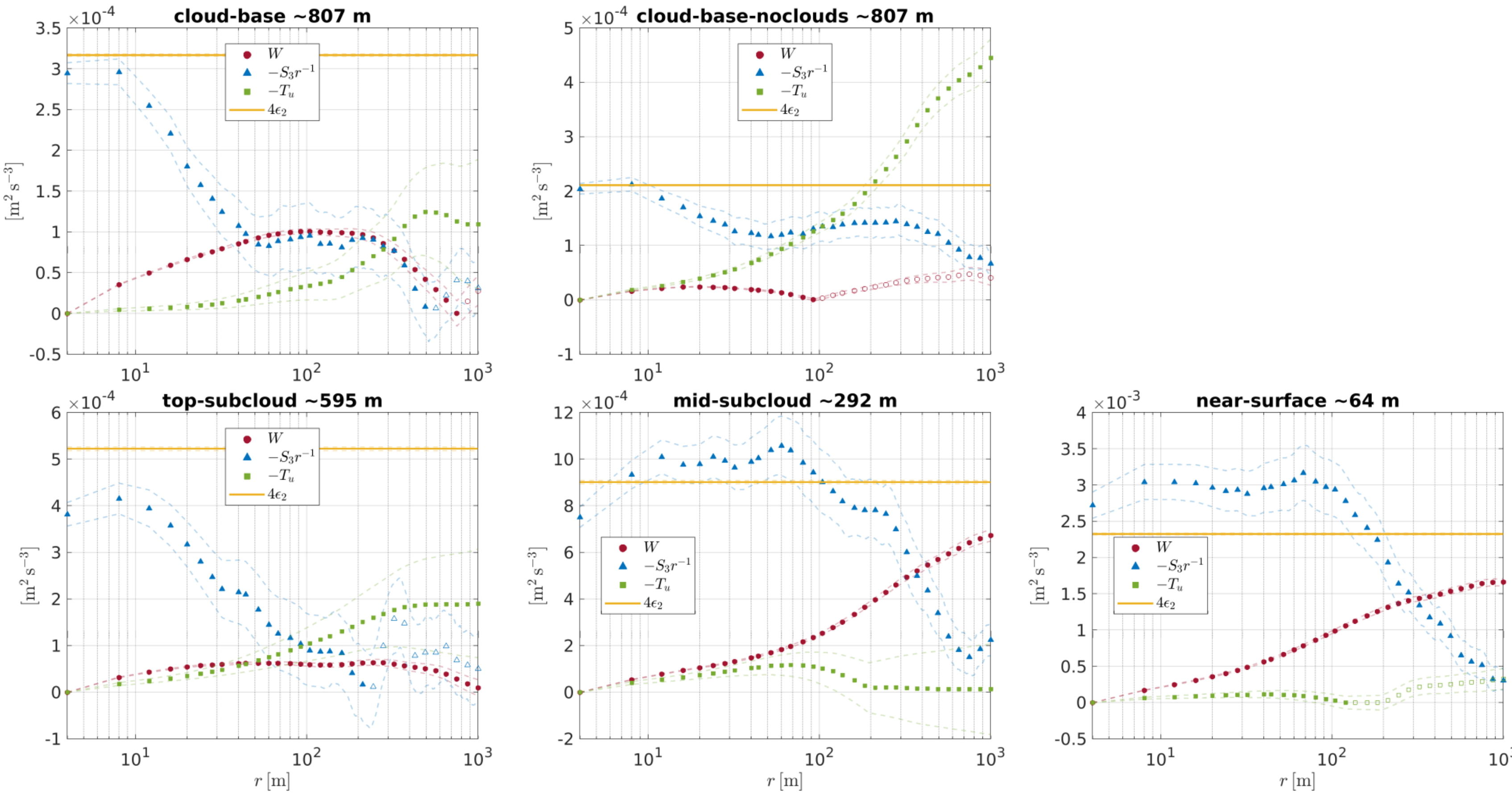

Total budget in linear scale